


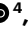








Temperature responses of ecosystem respiration

Shuli Niu ^{1,2}✉, Weinan Chen ^{1,2}, Liyǐn L. Liáng ³, Carlos A. Sierra ⁴, Jianyang Xia ⁵, Song Wang^{1,2}, Mary Heskell ⁶, Kaizad F. Patel⁷, Ben Bond-Lamberty ⁸, Jinsong Wang^{1,2}, Gabriel Yvon-Durocher⁹, Miko U. F. Kirschbaum ³, Owen K. Atkin¹⁰, Yuanyuan Huang¹, Guirui Yu ^{1,2} & Yiqi Luo ¹¹

Abstract

Terrestrial ecosystems release ~106–130 PgC yr⁻¹ into the atmosphere through respiration, counterbalancing photosynthetic carbon uptake and determining the strength of the land carbon sink. The effect of anthropogenic warming on the land carbon sink will depend on the temperature response of respiration. In this Review, we explore the relationships between temperature and ecosystem respiration from experimental and observational data at leaf, microbial, ecosystem and global scales. Contrary to the assumed monotonic increase in respiration with increasing temperature derived from Earth system models, empirical findings indicate a unimodal temperature response with a peak in respiration at an optimal temperature (T_{opt}). This unimodality is observed across a range of organization levels with T_{opt} values of 40–60 °C at the leaf and plant level, 11–46 °C at a microbial level and 6.5–33.3 °C at the global scale. Various mechanisms contribute to this unimodal pattern including enzyme deactivation, the thermodynamics of enzyme-catalysed reactions and changes in temperature-dependent factors such as soil moisture, nutrient availability and vegetation physiology. Incorporating the unimodality of these observed temperature responses of ecosystem respiration into Earth system models could facilitate attribution studies to identify the mechanisms responsible for the peaked response and increase the accuracy of carbon sequestration predictions.

Sections

Introduction

Temperature response of respiration

Multiscale evidence for unimodality

Model uncertainties and evaluations

Implications for carbon sequestration predictions

Summary and future perspectives

Introduction

Terrestrial ecosystems absorb $\sim 3.5 \text{ PgC yr}^{-1}$ from the atmosphere¹, offsetting around 30% of annual anthropogenic carbon dioxide (CO₂) emissions². However, coupled carbon–climate model projections under a business-as-usual emission scenario suggest that, by 2080, the respiratory CO₂ flux from the terrestrial biosphere will exceed the CO₂ uptake by photosynthesis, turning the terrestrial biosphere into a carbon source³. These projections assume that respiration increases sharply and monotonically with temperature, whereas photosynthesis increases more slowly and declines at high temperatures^{4,5}. Factors such as drought stress, fire, permafrost thaw and other factors could also contribute to future increases in terrestrial carbon losses^{6–8}. Although substantial progress has been made in developing Earth System Models (ESMs) that capture the fundamental processes that regulate the exchange of CO₂ between the biosphere and the atmosphere, substantial uncertainties remain in predictions of the temperature responses of photosynthesis⁹ and respiration¹⁰.

The Farquhar–von Caemmerer–Berry (FvCB) biochemical model¹¹ uses unimodal functions (functions with one maximum) to capture the temperature response of photosynthesis and has been incorporated into most ESMs; however, no comparable mechanistic model is yet available for the temperature response of ecosystem respiration¹². ESMs predominantly rely on monotonic functions such as Arrhenius-type functions or Q_{10} function, to describe the temperature response of respiration, projecting an exponential increase in respiration with climate warming. However, empirical evidence suggests that respiration follows a unimodal temperature response with the respiration rate reaching a maximum (R_{max}) at the optimal temperature (T_{opt}). Such responses are observed across various levels of biological organization, from single enzyme-catalysed reactions^{13,14}, the catalysed pathway of glycolysis¹⁵, the growth of organisms^{15–17} and microbial community respiration^{18,19}, to ecological processes such as leaf respiration^{20–23}, soil respiration^{24–26} and ecosystem respiration at the global scale²⁷. The discrepancy between models and observations implies that existing ESMs could overestimate rates of ecosystem respiration under anthropogenic warming.

The shapes and magnitudes of the monotonically increasing functions used to represent the temperature response of respiration varies between ESMs. Most models in the Coupled Model Intercomparison Project Phase 6 (CMIP6) use the Q_{10} function to describe the temperature response of heterotrophic respiration, but others use the Arrhenius equation²⁸. The Q_{10} factor used in these CMIP6 models varies from 1.45 to 2.61 (ref. 29), such differences lead to large intermodel variability in the predicted magnitude of heterotrophic respiration under a warming climate³⁰. Thus, understanding the temperature response of ecosystem respiration and its underlying mechanisms is central to improving model predictions of ecosystem responses to climate change.

In this Review, we synthesize evidence of unimodal temperature responses of respiration at different scales of organization and identify the mechanisms behind these phenomena. First, we summarize the functions used to describe the temperature response of respiration. Second, we outline unimodal temperature responses of respiration observed at different scales of biological organization. Third, we identify sources of uncertainty in the temperature response of ecosystem respiration projected by existing ESMs. Finally, we propose how the integration of unimodal temperature responses of ecosystem respiration into ESMs can improve predictions of respiratory fluxes.

Temperature response of respiration

The temperature response of respiration is influenced by multiple complex factors, such as the maximum catalytic activity of individual respiratory enzymes, availability of substrates and interactions with other environmental factors. The key theories and concepts used to describe these factors are outlined here.

Mathematical response functions

There are three function types that are often used to describe the observed and modelled temperature responses of respiration (Fig. 1a). Type 1 functions increase strictly monotonically and include exponential or exponential-like functions, such as the Arrhenius equation³¹, the equations of Lloyd and Taylor³² and Q_{10} functions³³. Type 2 functions increase monotonically and include a plateau. Type 3 functions are non-monotonic (unimodal) and reach R_{max} at T_{opt} .

These functions have different temperature sensitivities (Fig. 1b). Q_{10} factors are themselves measures of the relative temperature sensitivity, describing the factor by which respiration changes in response to a 10° change in temperature. The temperature sensitivity can also be assessed using the partial derivative of the temperature response function with respect to temperature (assuming that all other variables are constant). By this measure, the temperature sensitivity of exponential type 1 functions increases with increasing temperature. Type 2 functions have a maximum temperature sensitivity at intermediate temperatures, and temperature sensitivity approaches zero at high temperatures³⁴. The temperature sensitivity of type 3 functions is positive at temperatures below T_{opt} and negative above T_{opt} .

The thermodynamic theory has led to the derivation of a special set of type 3 functions^{14,26,35,36} that represent the temperature dependencies of enthalpy and heat capacity in molecular reactions (Supplementary Box 1). The unimodal properties of these thermodynamic functions support the idea that respiration could also have a unimodal temperature response. Laboratory-based measurements of soil and plant respiration at different temperatures have been used to test these thermodynamic functions, providing empirical support for this theory^{21,26}. However, it is not clear to what extent this enzyme-scale theory can be extended to ecosystem and global scales, which include multiple interactive components such as cycles of productivity and decomposition that interact with climatic drivers.

Apparent and intrinsic temperature responses

The temperature response of respiration observed in field measurements – known as the apparent temperature response – is a result of the combined effects of temperature and other environmental factors that vary with temperature on metabolic rates. For example, soil moisture changes as a function of temperature³⁷ with high temperatures frequently leading to reduced soil moisture, lower cell water content and potentially reduced respiration rates^{33,38} (Fig. 1c). To describe the apparent temperature response, an Arrhenius function representing the effect of isolated temperature changes on respiration can be combined with logistic functions representing the effect of changes in water and oxygen concentrations on respiration, yielding a unimodal function with a maximum respiration rate at specific temperatures and soil moistures^{33,38,39} (Fig. 1d). Understanding how temperature influences apparent respiration can help to quantify how the carbon released by ecosystems will change under climate change.

The direct effect of temperature on respiration when other temperature-varying environmental factors remain constant and non-limiting can be considered as the intrinsic temperature response^{40,41}.

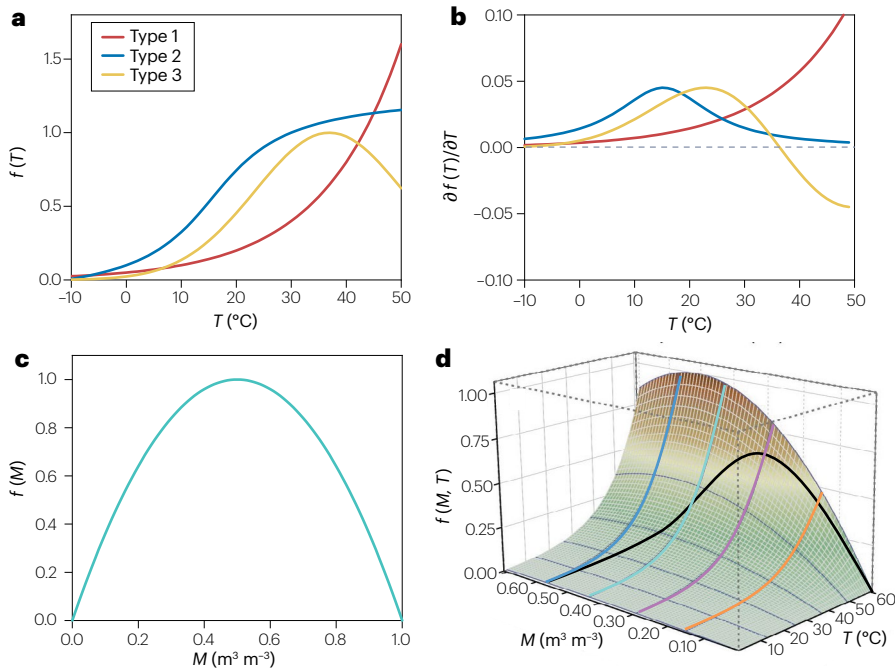


Fig. 1 | Temperature responses of respiration. **a**, Example type 1 (strictly increasing monotonic function), type 2 (increasing monotonic function with a plateau) and type 3 (non-monotonic function with a temperature optimum) functions to describe the intrinsic temperature response of respiration $f(T)$. **b**, The sensitivity of the intrinsic temperature responses of respiration in part **a** assessed using the first partial derivative of the functions assuming all other environmental variables are held constant. **c**, Proposed parabolic function $f(M)$ for the dependence of respiration on soil moisture M (refs. 143,144). **d**, A 3D surface representing the apparent temperature response of respiration $f(M, T)$ combining the type 1 $f(T)$ from part **a** and $f(M)$ from part **c**, including example responses to changing T with constant M (coloured lines) as well as a respiration function with both temperature and soil moisture changing together (black line). These three function types are often used to describe the temperature response of respiration, which can be influenced by other environmental factors such as soil moisture.

This intrinsic response is theoretical and is usually derived using attribution analysis of observed patterns or experimental manipulation. Insights on the intrinsic temperature response of respiration can reveal fundamental kinetic properties of the underlying biological processes and help to understand the mechanisms and links between respiration across different biological scales, and it can also be used to improve models of ecosystem respiration.

Thermal optimality

Asymmetric, unimodal response curves have been well characterized at low organization levels such as the temperature response of the metabolic and growth rates of enzymes, cells and whole organisms^{3,42}. Unimodal temperature responses of respiration typically rise gradually to a peak (R_{\max}) and then abruptly decline. For low organization levels (subcellular to whole organism), the temperature at which R_{\max} occurs is often described as an optimum (T_{opt}). The concept of an optimal temperature for the metabolic rate at these low organization levels arises from evolutionary theory. Evolution by natural selection represents an adjustment of traits that maximize the fitness of the individual to temperature change⁴³ and could promote traits that enhance the metabolic rate of whole organisms at a given temperature (T_{opt}).

At the ecosystem level, respiration represents the collective total metabolism of all organisms within an ecosystem. The temperature response of ecosystem respiration is driven by the various effects of biotic interactions (between organisms) and abiotic interactions (between organisms and their environment)²⁷ on the metabolism of each organism. Thus, the emergence of a peak in the temperature response of the ecosystem respiration is caused by the net effect of natural selection on all individuals within the ecosystem as well as the covariance of other environmental factors (such as water and nutrients) with temperature that could limit metabolic rates at high temperatures. Unlike the metabolic rate of whole organisms, the existence of an optimal rate of ecosystem respiration could be caused by factors

beyond a simple evolutionary temperature-driven optimization and remains poorly understood. Understanding the various mechanisms that contribute to the existence of a temperature optimum of ecosystem respiration will require the integration of processes across a range of levels of organization (sub-cellular to ecosystem) as well as diverse spatial and temporal scales.

Multiscale evidence for unimodality

Respiration can be measured using various techniques across a range of spatial and temporal scales, including leaf and soil chambers (1–10 cm in diameter), which monitor plant and soil respiration at timescales of minutes to days; eddy covariance towers (100–1,000 m in diameter), which monitor ecosystem–atmosphere carbon exchange to estimate ecosystem respiration rates at timescales of months to years; and flux networks, which monitor respiration rates across regions and continents (10–1,000 km) at temporal scales of years to decades. This section reviews empirical evidence from such measurements for the unimodality of the apparent temperature response of respiration at different levels of organization and examines the underlying processes.

Leaf-level and plant-level respiration

Leaves contribute roughly half of the respiratory flux of plants⁴⁴, with the remaining major fluxes coming from stems and roots, which are more difficult to measure in field settings. Leaf respiration rates are measured by monitoring the consumption of oxygen and/or the production of CO_2 by leaves in the dark, because in the light, measurement of O_2 and CO_2 fluxes is complicated by the concurrent fluxes produced by photosynthesis and photorespiration. Dark respiration consists of a suite of non-photorespiratory metabolic processes in the mitochondria that produce energy during the formation of ATP through oxidative phosphorylation and cycling of carbon metabolites via the tricarboxylic acid cycle, leading to the production of CO_2 as a by-product⁴⁵. Rates of CO_2 release by dark respiration at a given temperature can

differ between the day and night, owing to light-dependent inhibition of enzyme activity at multiple points along the respiratory pathway, as well as light-dependent removal of citrate from the tricarboxylic acid cycle to provide carbon backbones for nitrogen assimilation. Thus, the rate of respiration at a given temperature can decrease by around 25% throughout the night⁴⁶.

Approaches such as infrared gas analysis^{22,23,47,48} are widely used to monitor the temperature responses of leaf respiration. In this technique, a single leaf, or a small branch of needle-leaves, is inserted into a cuvette attached to the infrared gas analyser, and the cuvette temperature is changed to encompass a range of temperatures over a short time period^{22,47–50}. This approach makes it possible to obtain continuous and precise measurements of the CO₂ release associated with leaf respiration over a wide range of temperatures (0–65 °C) at intervals of <1 °C over short time periods (around 1 h), providing insight on the unimodal responses of leaf respiration to temperature, as well as insights into the temperature above which mitochondrial function begins to rapidly decline^{51,52}.

Temperature optima of leaf respiration have been detected widely based on observations in the dark using infrared gas analysis⁴⁷. For example, infrared gas analysis measurements of *Quercus macrocarpus* revealed that relative changes in leaf respiration rates increase more slowly at temperatures above 30 °C (Fig. 2). Thus, the calculated Q₁₀ values decrease by 20–30% as the leaf temperature increases from 20 °C to 40 °C (refs. 22,47,49,51). The efficiency of enzymes increases with increasing temperatures within the range of growth temperatures

(usually <40 °C) that plants are adapted to, leading to an increase in respiration rates. However, the rate of photosynthesis decreases with increasing temperatures above its optimal temperature; therefore, at temperatures above this temperature optima (typically above 30 °C), the lack of substrates such as sugar and starch, which are produced by photosynthesis, begins to limit the rate of respiration, despite a continued need for maintenance respiration to provide energy for the plant cells^{51–55}. Thus, reduced substrate supplies at high temperatures can contribute to the observed unimodal temperature response.

The interaction of multiple processes causes leaf respiration to suddenly increase with increasing temperature before rapidly declining at temperatures above T_{opt} . At temperatures in the range of 40–50 °C, plants can experience severe heat stress leading to increased production of reactive oxygen species, increased rates of alternative oxidase engagement, reduced cytochrome oxidase activity, the production of heat shock proteins, the destabilization of phospholipid membranes and protein denaturation^{23,55–57}. These co-occurring processes can lead to a respiratory burst (Fig. 2), in which respiration rates increase to R_{max} . At temperatures above T_{opt} , respiration rates quickly decrease because cells and enzymes lose functional stability at these extreme temperatures, leading to cellular failure and enzyme deactivation^{22,23,55,57}.

Environmental and biological variables also contribute to variability in T_{opt} and R_{max} (refs. 56,57). Increased availability of sugar and starch substrates produced by photosynthesis can increase T_{opt} by prolonging the pre-burst respiratory stage before the onset of cellular

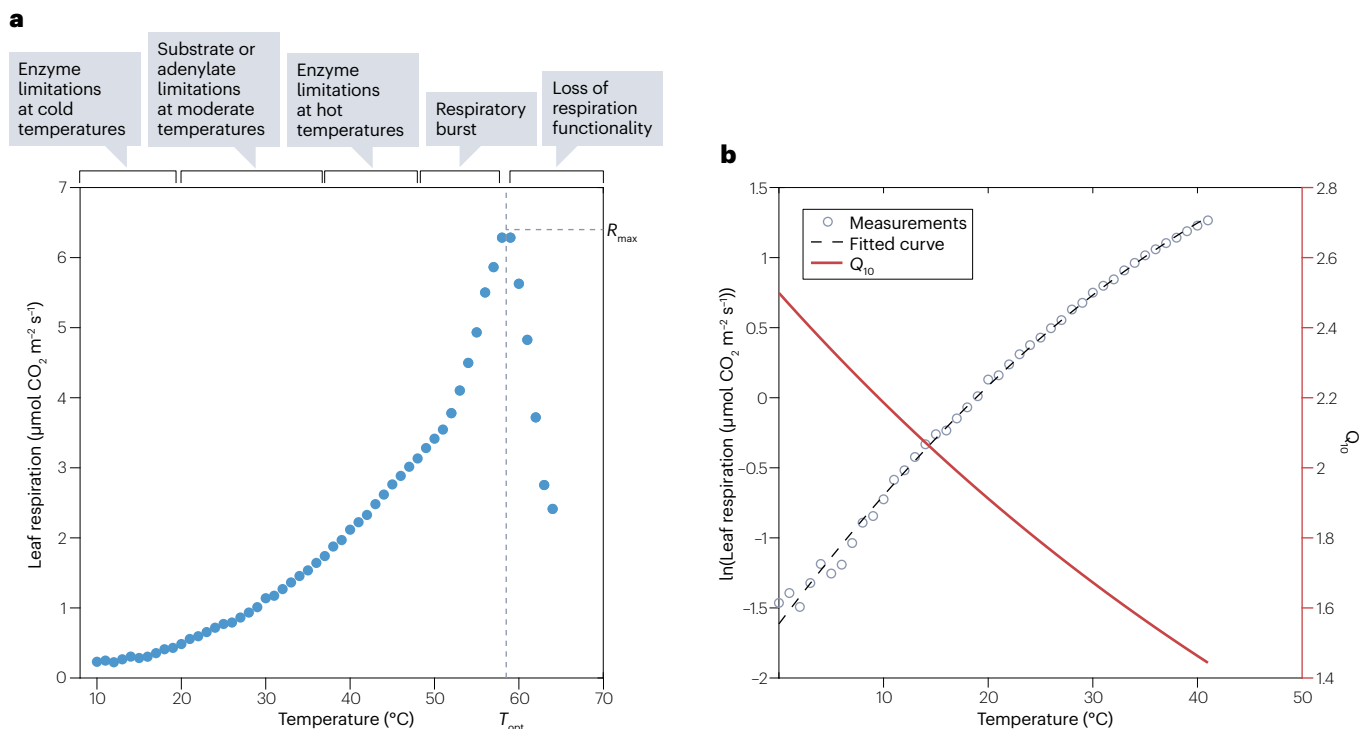


Fig. 2 | Short-term temperature response of leaf respiration. a, On the basis of refs. 51,55, the temperature (T) response of respiration (R) measured for *Quercus macrocarpus* (unpublished data M.H.), identifying the regions in which the response is controlled by enzymatic or substrate limitations, a respiratory burst, a peak at the maximum respiration (R_{max}) and a subsequent decrease in respiration at temperatures above the optimal temperature (T_{opt}) caused by

cellular failure. **b**, The measured respiration rates (open circles) in part a at temperatures under 50 °C before the respiratory burst plotted on a log scale and fitted with a second-order polynomial ($\ln R = -0.0007T^2 + 0.117T - 2.66$) (black line), which was used to obtain the corresponding Q_{10} function (red line). Leaf respiration accelerates with increasing temperature until it peaks and then decreases rapidly owing to cellular failure and enzyme deactivation.

failure, increasing the resilience of the plant to extreme heat^{56,57}. Seasonal thermal acclimation (that is, metabolic adjustments to sustained changes in growth temperature) can lead to R_{\max} and T_{opt} of leaves being higher in winter than in summer because the leaf energy metabolism is more heat-tolerant in trees experiencing ice encasement in winter than in warmer summer conditions²². For example, R_{\max} and T_{opt} of snow gum (*Eucalyptus pauciflora*) trees increased from 20 $\mu\text{mol CO}_2 \text{ m}^{-2} \text{ s}^{-1}$ and 54 °C in summer to 23 $\mu\text{mol CO}_2 \text{ m}^{-2} \text{ s}^{-1}$ and 57 °C in winter, respectively²². Other environmental factors that can influence T_{opt} and R_{\max} include latitude, with T_{opt} declining with increasing latitude²³, and leaf nitrogen and phosphorus abundance, with R_{\max} increasing with increasing N and P availability⁵⁸.

Experimental evidence is continuing to improve understanding of the temperature response of leaf respiration, especially at temperatures close to T_{opt} . Understanding the response of respiration to rising temperatures will become increasingly important as climate change causes plants to experience extreme heat more frequently. Additionally, plant respiration is a major component of the global carbon cycle; therefore, to project how the terrestrial biosphere carbon sink will change with increasing temperatures ESMs must include accurate representations of the temperature response of plant respiration.

Soil respiration

Soil respiration is primarily the sum of heterotrophic respiration, which mineralizes soil organic matter, and plant root respiration. Chambers can be used to measure soil respiration in the field by enclosing a specific area of soil within a sealed container and measuring the accumulation of CO_2 . Heterotrophic respiration can be estimated in the field by measuring the CO_2 flux of soil without living roots, either by girdling trees (in which bark and procambial layers are removed) or by using exclusion plots in which the roots have been cut (trenching)⁵⁹. Alternatively, heterotrophic respiration can also be measured in the laboratory using soil incubation, whereby collected soil samples are kept under controlled conditions to measure CO_2 production rates over a specified period. Meanwhile, plant root respiration is almost never measured directly but calculated by subtracting heterotrophic respiration from the total soil respiration⁶⁰. Heterotrophic and root respiration respond differently to changing temperatures^{61–63} owing to the different drivers and organisms involved. The temperature responses of these respiration rates are determined by multiple processes, including evolutionary adaptation, microbial community changes^{64,65}, physiological changes^{66,67} and changes in the available carbon inputs and substrate pools^{68–71}.

Unimodal temperature responses of heterotrophic respiration have been reported widely since the 1980s, and the T_{opt} values can vary between locations owing to changes in community composition and environmental factors^{72,73}. T_{opt} of heterotrophic respiration is often calculated from temperature response curves measured in laboratory-based incubations with soils incubated at different temperatures for days to months with values ranging from 11 °C to 46 °C or even higher^{19,26,73–77}. This broad range likely reflects the variability of the microbial populations and communities between the locations from which soil samples were taken. Climate also has a substantial impact on T_{opt} (refs. 19,77); for example, the T_{opt} of soil samples from Long-Term Ecological Research sites across the USA varied from 28–29 °C for taiga and temperate soils to 37 °C for tropical soils⁷⁷. This variability was attributed to differences in the composition and function of microbial communities between the locations because the tropical soils had

thermo-tolerant microorganisms, whereas taiga communities could not survive at higher temperatures.

Although declines in soil respiration rates have been observed at soil temperatures above 25 °C in a global synthesis of 27 warming experiments²⁴, field measurements of total soil respiration rarely report a T_{opt} value. There are three potential reasons for the lack of reported T_{opt} values. First, soil respiration represents a mix of carbon derived from belowground carbon allocation, net primary production, root respiration and heterotrophic respiration. Each of these components can have a different temperature response and T_{opt} value, making it difficult to attribute changes in soil respiration to changing temperatures⁷⁸. Second, exponential models are often used to fit soil respiration data, which assume that Q_{10} is constant at all temperatures and thus has no peak⁴. Third, measuring T_{opt} in the field requires the presence of severe environmental stress such as drought. It is also possible that organisms do not often experience temperatures above their T_{opt} in field conditions because soils can provide a buffer against high air temperatures^{74,79}. However, laboratory-based measurements of soil samples collected from different elevations revealed a unimodal response for soil respiration at temperatures above 35 °C, irrespective of the changes in climate across elevations⁷⁵.

Unimodal temperature responses of soil respiration have not yet been incorporated into most land carbon cycle models. Nevertheless, there have been promising developments. For instance, the Dual Arrhenius and Michaelis–Menten (DAMM) kinetics model incorporates temperature-sensitive enzymatic processes with critical constraints related to soil water content and substrate supply to simulate soil respiration²⁹. A unimodal temperature response emerges in DAMM owing to the interaction of the Arrhenius equation with functions that depend on soil moisture and oxygen levels. Furthermore, the macromolecular rate theory (MMRT)^{5,14,80,81} has also been developed based on the thermodynamics of enzyme-catalysed reactions and provides theoretical support for describing the unimodality of the intrinsic temperature response of soil respiration⁸⁰.

Future work could leverage and/or integrate DAMM and MMRT by replacing the Arrhenius equation in DAMM with MMRT. Such advances could help to elucidate the thermodynamic properties of enzymes involved in respiration and help to interpret emerging observations of unimodal temperature responses of heterotrophic respiration. Additionally, future research should seek to integrate models with data from experiments that exclude confounding environmental factors to isolate causality between temperature and soil respiration, reduce uncertainties in the temperature responses of soil respiration and develop models that accurately capture the effects of global environmental change on soil respiration⁶⁰.

Ecosystem respiration

Ecosystem respiration integrates plant and soil processes and is affected by many confounding factors; therefore, the temperature dependence of ecosystem respiration is more complex than that of its components⁸². Eddy covariance towers can directly measure the net ecosystem exchange of CO_2 between the biosphere and the atmosphere, which can be partitioned into gross primary production and ecosystem respiration using night-time-based or daytime-based algorithms^{83,84}. The inferred ecosystem respiration can reveal the intricate dynamics of respiratory CO_2 at the ecosystem level and how it responds to changing environmental conditions such as changes in temperature over months to years.

Type 1 monotonic functions are often used to fit the temperature responses of ecosystem respiration obtained from eddy covariance measurements of different ecosystem types, and the Q_{10} value is used to quantify this temperature dependence^{85–87}. In early-generation models, the Q_{10} value was often treated as a constant (typically 2)^{3,85}. However, the Q_{10} value of the apparent temperature response of ecosystem respiration substantially varies with time, location and temperature^{88–90}. For example, in an alpine meadow, the apparent Q_{10} value decreased from 4.34 in the control to 2.92 under warming treatment⁹¹. This variability does not arise solely from the effects of temperature but also from the effects of temperature-dependent variables such as soil moisture^{92,93}, biomass or productivity⁹⁴ and litter input⁹⁵. These biological and abiotic factors alter soil microbial activities and plant productivity and regulate substrate availability, influencing multiple processes in ecosystem respiration^{40,96–98}.

Field evidence suggests that exponential response curves do not adequately represent the mechanisms underlying the temperature response of ecosystem respiration. The inhibition of plant respiration and soil respiration at temperatures above a T_{opt} value has been observed for various ecosystems^{22,47,52,73,75,99–102}, suggesting that unimodal functions could adequately describe field observations of the response of ecosystem respiration to increasing temperature. However, it can be difficult to disentangle the processes and mechanisms underlying this response in natural ecosystems. For example, the apparent T_{opt} obtained from eddy covariance measurements varies with vegetation type, soil moisture, substrate supply and nutrient availability with values ranging from 15 °C to 30 °C (refs. 93,94,103) (Fig. 3).

The potential mechanisms underlying the unimodality of the temperature response of ecosystem respiration could arise from the individual or combined effects of multiple processes. First, enzyme activities and metabolic rates could be inhibited at high temperature^{73,104}. Second, the decreasing affinity of the enzyme for the substrate

with increasing temperatures could counteract the concurrent increase in enzyme activity, leading to the functionality of the enzyme having no net temperature dependence⁴. Third, decreasing Q_{10} values with increasing temperatures could contribute to the slow increase (or even decrease) in respiration at high temperatures¹⁰⁵. Fourth, water limitation and dryness concomitant with high temperatures could lead to reduced respiration rates^{93,106,107}. Finally, declines in photosynthetic rates at high temperatures could reduce the respiratory substrate supply, constraining ecosystem respiration^{108–110}. These processes and mechanisms interact with each other and are difficult to disentangle in real ecosystems. Thus, the role of these mechanisms in determining the presence of a peak in the apparent temperature response of ecosystem respiration remains uncertain.

Global network of observations

FLUXNET is a global network of long-term carbon flux measurements that enables ecosystem respiration data to be compared between sites or ecosystems¹¹¹. Established in the late 1990s, FLUXNET provides standardized ecosystem-scale data on net ecosystem exchange and ecosystem respiration as well as corresponding meteorological and biological measurements of factors such as the vegetation type and dominant species from each location¹¹². The FLUXNET2015 data set released in 2020 includes 212 sites around the globe, covering a large area and most vegetation types, with more than 1,500 site-years of data¹¹². The long-term, high-frequency eddy covariance flux data from FLUXNET can be synthesized over time and space to explore ecosystem respiration across regional-to-global scales¹¹¹.

The response of ecosystem respiration to temperature is affected by various biotic and abiotic factors that covary with temperature⁴. Empirical observations can only measure Q_{10} values of the apparent temperature response, and it is challenging to infer a Q_{10} value of the intrinsic temperature response of ecosystem respiration from

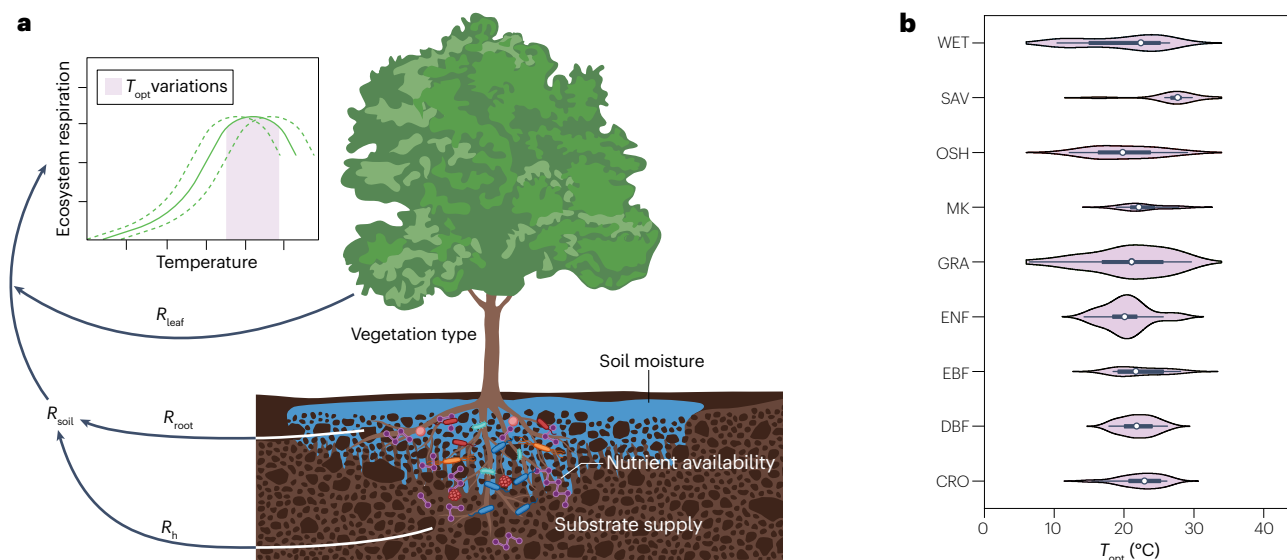


Fig. 3 | Variation of the optimal temperature of ecosystem respiration. **a**, Factors that influence the rate of soil respiration R_{soil} (sum of the root respiration R_{root} and heterotrophic respiration R_h) and the rate of leaf (R_{leaf}) respiration, leading to variations in the temperature response of ecosystem respiration and a range of optimal temperatures (T_{opt} , shaded red region in the inset). **b**, The range of observed T_{opt} values for wetland (WET), savanna (SAV), open

shrublands (OSH), mixed forest (MF), grassland (GRA), evergreen needle-leaf forest (ENF), evergreen broadleaf forest (EBF), deciduous broadleaf forest (DBF) and croplands (CRO)²⁷. The box plots indicate the median values, interquartile range and the 5th and 95th percentiles. The violin plot indicates the full data distribution. The apparent T_{opt} varies with vegetation type, soil moisture, substrate supply and nutrient availability.

observational data, which is subject to the confounding effects of covarying factors. Therefore, assessments of the global-scale temperature response of ecosystem respiration using FLUXNET data sets have mainly focused on the variation of the apparent Q_{10} values of ecosystem respiration between sites and years^{41,105}. However, flux site observations in which confounding effects were minimized by using the scale-dependent parameter estimation methodology proposed an intrinsic Q_{10} value of ecosystem respiration of around 1.4, which is independent of mean annual temperature and biomes⁴¹. Data from 74 FLUXNET sites spanning diverse climates and biomes indicated that warming reduces apparent Q_{10} values more in colder regions than in other locations¹⁰⁵. Therefore, future warming could homogenize the Q_{10} values of the apparent temperature response of ecosystem respiration across biomes.

The decrease of apparent Q_{10} values with increasing temperatures could result in the emergence of a peak in the temperature response of ecosystem respiration. In 2023, evidence for the widespread existence of a peaked apparent temperature response of ecosystem respiration was observed by analysing FLUXNET2015 data sets for 212 sites²⁷. Unimodal temperature response curves for ecosystem respiration were observed at 183 of these sites with T_{opt} varying between ecosystems with a range of 6.5–33.3 °C. Across the different biomes, savanna has the largest T_{opt} of 27.8 ± 0.5 °C, whereas wetlands have the smallest T_{opt} with a value of 19.6 ± 1.4 °C (Fig. 3). These observations revealed a linear increase in T_{opt} with annual maximum daily temperature, suggesting that ecosystem respiration adapts to changes in temperature through shifts in T_{opt} across different sites and vegetation types. This theory is in contrast to the traditional understanding that the thermal adaptation of ecosystem respiration occurs through adjustments in temperature sensitivity and basal rate^{51,113–117}.

Given the decline in ecosystem respiration at temperatures above T_{opt} , it is important to explore changes in the temperature sensitivity before and after the peak. Further work is needed to explore how the maximum temperature sensitivity changes between biomes and as a function of time and what mechanisms are responsible for these differences. Such insight could help to improve simulations of climate change–carbon cycle feedbacks and develop better respiration models.

Model uncertainties and evaluations

Accurate representations of ecosystem respiration in ESMs can elucidate the feedback mechanisms governing climate change and underscore the resilience of ecosystems to an evolving environment. This section outlines the uncertainties in existing CMIP models and compares modelled and measured T_{opt} to identify ways in which existing models could be improved.

CMIP model uncertainties

CMIP models determine ecosystem respiration based on the size of each carbon pool, carbon residence time of each pool, carbon transfers between different pools and environmental scalars modifying decomposition rates of soil organic carbon¹¹⁸. These models have greatly improved predictions of the land carbon cycle, reducing the uncertainty of the vegetation productivity and ecosystem carbon stock¹¹⁹. However, there are large variations in the carbon storage capacity and respiration of soils predicted by CMIP models, and these predictions do not agree with observed values^{28,120}. For example, CMIP5 and CMIP6 underestimate the carbon residence times of terrestrial ecosystems by 34.1% and 29.5%, respectively¹¹⁹. Therefore, it remains unclear whether

the underestimation of carbon residence time is a major source of uncertainty in the projection of ecosystem respiration by ESMs.

It is important to consider whether incorporating a unimodal temperature response could reduce the uncertainty of model projections of ecosystem respiration. To answer this question, it is first necessary to determine whether and how the temperature dependence of ecosystem respiration varies between existing ESMs. Second, if temperature dependence of ecosystem respiration is a critical contributor to CMIP model uncertainties, some ESM models must be refined with improved temperature functions or by considering co-limiting factors to capture the presence of a peak ecosystem respiration. Finally, if some CMIP models capture the unimodal temperature response of ecosystem respiration, they can be used to explore the process-based mechanisms responsible for observed temperature responses.

The temperature response functions used to model autotrophic respiration and heterotrophic respiration vary substantially between process-based models. In most models, temperature regulates the maintenance respiration component of autotrophic respiration rather than growth respiration^{12,121}. For example, plant maintenance respiration is simulated as a linear function of temperature for each plant carbon pool in the ORCHIDEE model¹²², whereas growth respiration is assumed to be constant as a function of remaining allocatable biomass. In the JULES and Uvic models, plant maintenance respiration is simulated as the product of a dark respiration coefficient and the maximum rate of carboxylation of Rubisco (ribulose-1,5-bisphosphate carboxylase/oxygenase), which is constrained by temperature¹²³. Other models, such as CLM5 (ref. 124), use a Q_{10} function to simulate the temperature dependence of maintenance respiration in different plant tissues.

Only 2 out of 16 CMIP5 models (BCC-CSM1.1 and GFDL-ESM2G) use a unimodal temperature response function to simulate the temperature response of heterotrophic respiration²⁹, with most models using Q_{10} or Arrhenius functions instead. Unfortunately, the temperature response functions remained unchanged in most ESMs when updating from CMIP5 to CMIP6 (ref. 28). Thus, variations in the choice of functions used to simulate the temperature dependence of autotrophic and heterotrophic respiration could be an essential contributor to the large spread of ecosystem respiration values projected across the ESMs¹²⁵. Approximately two-thirds of the intermodel variability in predictions of ecosystem respiration is caused by differences in the function used to simulate the temperature response³⁰. Additionally, the effects of interactions between temperature response and soil moisture, and other environmental variables on CMIP projections of respiration have not yet been explored. Furthermore, ESMs need to better link gross primary productivity with substrate supply for autotrophic respiration over short timescales (minutes to days) by simulating a dynamic photosynthate supply for respiration and also improve the link with heterotrophic respiration over medium timescales (days to seasons)¹²⁶. Understanding these interactions is crucial for determining the apparent temperature response of respiration in these models.

Model evaluations

CABLE is a widely used global land-surface model that can simulate the temperature response of ecosystem respiration to allow the comparison of modelled and measured T_{opt} values. In the CABLE model, respiration is simulated with Q_{10} functions and is indirectly affected by photosynthate supply, which is regulated by the leaf senescence rate¹²⁷. CABLE simulations driven by CRUNCEPv7 meteorological forcing were used to calculate daily ecosystem respiration and temperature during 2000–2013 (ref. 128). CABLE was chosen instead of CMIP because

Glossary

Apparent temperature response

The overall observed or measured changes in respiration rate as a function of temperature, including the effects of external factors such as soil water content, substrate and nutrient supply, which also vary with temperature.

Autotrophic respiration

Respiration from plant growth and maintenance.

Ecosystem respiration

The release of CO₂ into the atmosphere from the collective metabolic processes of living organisms within an ecosystem.

Heterotrophic respiration

Respiration from the decomposition of litter and soil organic matter by soil microorganisms.

Intrinsic temperature response

The isolated effect of temperature on respiration rate, assuming all covarying factors remain constant. It is obtained

from field or laboratory experiments in which all environmental factors except temperature are held constant and non-limiting.

Optimal temperature

T_{opt} . The temperature at which the rate of respiration is maximized.

Q_{10} factor

The factor by which the respiration rate changes for a 10° change in temperature, used as a measure of the relative temperature sensitivity.

Q_{10} function

A strictly monotonic increasing function used to describe the temperature response of respiration as $f(T) = ae^{bT}$, in which T is the temperature, a is a fitted constant and $b = \ln(Q_{10})/10$.

Temperature sensitivity

The change of respiration per unit change in temperature in the apparent or intrinsic temperature response of respiration.

current CMIP models only provide monthly outputs for ecosystem respiration, which are difficult to compare with daily observations of ecosystem respiration. By fitting the simulation results with different types of functions and selecting the best fitting, three types of functions emerged for the apparent temperature response of ecosystem respiration.

The simulated values were compared with FLUXNET data measured at the location corresponding to the site simulated by CABLE (Fig. 4), and the best fitting function for the observed data was similarly identified. This model–observation comparison revealed at least three differences. First, the temperature responses of respiration simulated by CABLE were type 1 functions for most terrestrial ecosystems (147 out of the 212 sites), whereas FLUXNET data were dominated by type 2 and 3 functions (155 out of the 212 sites). Second, despite being coded with Q_{10} functions, CABLE can generate type 3 responses to a limited extent and exhibited type 3 response curves at 29 of the 212 sites. However, the modelled and observed T_{opt} values for a single location were quite different, for example, FLUXNET data at the site of Australia Dry River indicated a T_{opt} value of 28.5 °C, whereas CABLE produced a value of 22.6 °C (Fig. 4i). Third, the simulated ecosystem respiration was substantially different from that observed at the same temperature even in locations with the same function type (Fig. 4a,e,i). Thus, further attribution research is needed to understand the mechanisms behind observed temperature responses of respiration and improve simulations.

The mismatches between the modelled and measured temperature responses of ecosystem respiration are likely to be caused by three factors. First, the functions for the apparent temperature response of ecosystem respiration in real-world ecosystems are likely different from the Q_{10} function used in CABLE or other monotonic functions used in ESMs. Second, the observed unimodal temperature response of respiration at the ecosystem scale probably arises from interactions among temperature, moisture and other factors, which are not accounted for in CABLE. Therefore, further experiments are necessary to distinguish the effects of these factors on ecosystem respiration. Third, the function parameters identified from observations are likely to vary between locations. Therefore, parameters representing properties of ecosystems¹²⁹ must vary spatially and temporally to allow global models to accurately simulate ecosystem dynamics^{130–132}.

The mechanisms driving the observed unimodal temperature responses of respiration can be identified using various attribution approaches, some of which have already been applied to carbon cycle research. For example, a Bayesian framework with a data assimilation technique was used to identify the most probable function to represent heterotrophic respiration from lignin decomposition from three candidate functions (that is, first-order, Michaelis–Menten and logistics)¹³³. Additionally, four models (a conventional first-order kinetic decomposition model, an interactive two-pool model, a Michaelis–Menten model and a reverse Michaelis–Menten model) to represent the microbial priming effect observed in 84 data sets of isotope-labelled soil respiration were evaluated using the Bayesian framework¹³², with the interactive two-pool model being identified as the most effective. Moreover, a deconvolution analysis¹³⁴ suggested that fast carbon transfer processes, such as root exudation, are of minor importance in determining the response of soil surface respiration to a step CO₂ increase, whereas fine-root turnover is a major process, adding carbon to the rhizosphere under elevated CO₂. Some of these methods can also be used to identify mechanisms driving observed temperature responses of respiratory processes to improve the predictive ability of ESMs¹²⁵.

Implications for carbon sequestration predictions

The increase in ecosystem respiration with increasing temperatures projected by many existing ESMs could lead to positive feedback between anthropogenic warming and ecosystem carbon cycling¹³⁵. If warming amplifies the release of carbon through ecosystem respiration more than carbon uptake through photosynthesis, atmospheric CO₂ levels could increase, exacerbating the warming. However, the unimodal temperature responses of respiration observed across various scales imply that the terrestrial ecosystem respiration rates might peak and possibly decline instead of continuing to rise at supra-optimal temperatures. Therefore, the current generation of ESMs that mostly project monotonic increases in ecosystem respiration with warming could overestimate the amount of carbon released by terrestrial ecosystems. Thus, to improve projections of climate–carbon cycle feedback, ESMs must be modified to include the unimodal temperature response of ecosystem respiration.

The unimodal temperature response of ecosystem respiration can also lead to regional and seasonal differences in the effect of warming on ecosystem respiration. The change in carbon release rates per unit change of temperature is larger in cold climates than in warm climates; thus, ecosystem carbon release in cold climates is strongly influenced by increasing temperatures. For instance, in permafrost regions, which store large amounts of carbon, increasing temperatures in the cold season could cause more soil carbon losses than in the warm season^{136,137}.

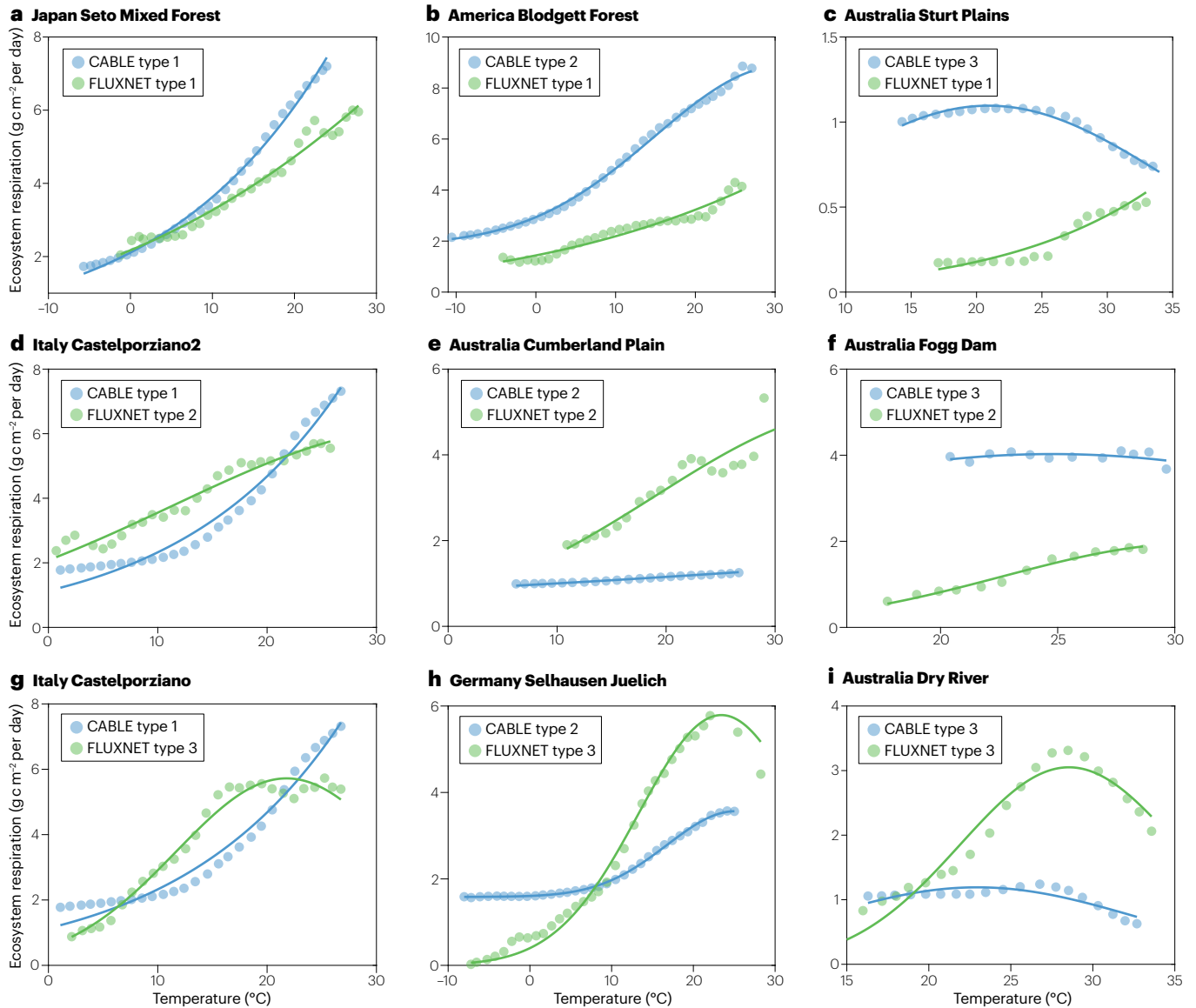


Fig. 4 | Comparing the observed and modelled temperature responses of ecosystem respiration. **a–c**, Examples of FLUXNET data (green markers) in three locations where the observed temperature response of ecosystem respiration follows a type 1 function (monotonic increase with temperature) compared with the output from the CABLE Earth system model¹²⁸ at the corresponding site coordinates (blue markers), which follows a type 1 (part **a**), type 2 (part **b**), monotonic increase with temperature until reaching a plateau) or type 3 (part **c**,

non-monotonic pattern with a distinct peak) function. The green and blue lines are the regression lines fitted to the data, which were used to identify the function types. **d–f**, As in parts **a–c**, but in locations with type 2 functions describing the FLUXNET data. **g–i**, As in parts **a–c**, but in locations with type 3 functions describing the FLUXNET data. The CABLE model cannot accurately simulate the temperature optima of ecosystem respiration found in observational data.

In warm climates, limited availability of water, nutrients and other resources could constrain the response of ecosystem respiration to changes in temperature. At high temperatures, heat stress could lead to irreversible decreases in the rate of respiration under further temperature increases. However, the interaction of some abiotic processes (such as desorption) with biotic processes could accelerate carbon losses under warming^{138,139}. At high temperatures, desorption reaction rates might increase the pools of active enzymes and labile carbon, increasing respiratory CO₂ (refs. 138,139). Mapping global variations

in T_{opt} values of ecosystem respiration could help to identify regions that are vulnerable to climate warming. Additionally, ESM carbon cycle and climate change forecasts could be improved by accounting for regional and seasonal differences in the temperature sensitivity of ecosystem respiration.

Summary and future perspectives

Understanding the temperature dependence of ecosystem respiration is crucial for accurately predicting the future land carbon sink under a

warming climate. The current generation of ESMs predominately relies on Q_{10} functions to describe the temperature response of respiration. However, widespread unimodal temperature responses of respiration have been observed at different scales from leaf and microbial scales to ecosystems and the globe, with global ecosystem T_{opt} values varying from 6.5 °C in cold regions to 33.3 °C in warm regions. This observed unimodal pattern contradicts the monotonic increase in respiration with increasing temperature predicted by current ESMs. This section outlines a research roadmap to advance understanding and improve model predictions of the response of ecosystem respiration to changes in temperature.

First, it is essential to systematically monitor respiration at different scales. High-quality data from field and controlled experiments are needed to improve modelling estimates of ecosystem respiration. Advances in measurement techniques, such as high-resolution temperature-controlled cuvettes, have provided insights into the response of leaf respiration to a broad range of temperatures experienced during growth and at high extremes^{22,23,47}. Although such experiments have covered numerous diverse species and biomes, many regions such as Asia and Africa^{47,102,140} remain under-represented. Additionally, under-represented plant species, including C4, CAM, non-tree and understory plant species, require further study. Experimental approaches focusing on environmental and biological changes are also needed to yield insight into the mechanistic control of respiration. Meanwhile, the extent to which temperature is responsible for changes in nocturnal respiratory CO₂ release should also be further explored⁴⁶. Furthermore, as global temperatures climb and become increasingly variable, it will be especially important to understand how heat waves influence the temperature response of respiration^{55,141}.

Next, ESMs that can replicate the observed unimodal response of ecosystem respiration and the associated T_{opt} values are urgently needed to improve predictions of the climate–carbon cycle feedback. First, the temperature response functions of respiration should be derived from observations and used to improve model structures by enhancing the representation of the unimodality and constrain model parameters via data assimilation¹²⁹. Second, temperature gradient experiments are needed to improve process-based modelling of autotrophic and heterotrophic respiration and their thermal responses. Third, the representation of the effects of factors such as moisture must be incorporated into ESMs to improve respiration simulation at high-temperature conditions. Models should also incorporate mechanisms or phenomena, such as carbon–nutrient interactions and tree mortality under climatic extremes, to improve modelling of ecosystem respiration because these issues are poorly constrained in ESMs. Fourth, the intrinsic processes driving the observed temperature response of ecosystem respiration should be identified using attribution analysis, inverse modelling, machine learning or a combination of them (such as hybrid modelling)¹⁴². Finally, interdisciplinary collaborations are needed to bridge the gap in scales among experiments, field observations and ESM grid cells.

Moreover, mechanisms underlying the unimodal temperature response of ecosystem respiration need to be further revealed in future studies. It remains unclear whether these mechanisms can be directly scaled from the cellular, individual level to the entire ecosystem, or they arise from the interplay of natural selection acting on individuals with their surrounding environment. In addition, the temperature dependence of ecosystem respiration is not static. It changes with temporal scales of observation through acclimation, adaption and evolution²⁷. Anthropogenic warming is a gradual process and occurs

over timescales commensurate with diverse ecological and evolutionary phenomena. Thus, the T_{opt} value of ecosystem respiration could change with time and space²⁷, influencing predictions of future ecosystem respiration under climate warming. Therefore, the changes of T_{opt} and its controlling factors must be comprehensively explored further. Field observations, manipulative experiments and ecosystem modelling must be coordinated to improve measurements of T_{opt} values for ecosystem respiration across scales and understand the factors controlling the T_{opt} values.

The intricate interconnections between myriad factors and processes in Earth systems pose a complex challenge for research and often require some initial simplification before they can be modelled. In process-based models, the intrinsic temperature response of respiration interacts with other temperature-induced changes (such as substrate availability, drought stress, fire and permafrost thaw) to reproduce the apparent temperature response of respiration. Separating the intrinsic temperature response of respiration from the effects of the confounding factors is essential to enable ESMs to accurately attribute outcomes and improve understanding of the complex reality of respiration changes under future climate warming. Therefore, further work is needed to study the intrinsic temperature response of respiration and overcome the experimental difficulties associated with controlling the other factors. However, for ESMs to achieve realistic simulations of the apparent temperature response of respiration, the representation of the response of other components (such as water and nutrients) to changes in temperature must also be improved alongside representations of the intrinsic temperature response of respiration.

Data availability

The data for Fig. 2 are available from M.H. The observational data used to make Fig. 4 were obtained from FLUXNET data sets (<https://fluxnet.org/>).

Published online: 16 July 2024

References

1. Friedlingstein, P. et al. Global Carbon Budget 2022. *Earth Syst. Sci. Data* **14**, 4811–4900 (2022).
2. *Climate Change 2022 — Mitigation of Climate Change: Working Group III Contribution to the Sixth Assessment Report of the Intergovernmental Panel on Climate Change* (Cambridge Univ. Press, 2023). <https://doi.org/10.1017/9781009157926>.
3. Cox, P. M., Betts, R. A., Jones, C. D., Spall, S. A. & Totterdell, I. J. Acceleration of global warming due to carbon-cycle feedbacks in a coupled climate model. *Nature* **408**, 184–187 (2000).
4. Davidson, E. A., Janssens, I. A. & Luo, Y. On the variability of respiration in terrestrial ecosystems: moving beyond Q_{10} . *Glob. Change Biol.* **12**, 154–164 (2006).
5. Duffy, K. A. et al. How close are we to the temperature tipping point of the terrestrial biosphere? *Sci. Adv.* **7**, eaay1052 (2021).
6. Hugelius, G. et al. Large stocks of peatland carbon and nitrogen are vulnerable to permafrost thaw. *Proc. Natl Acad. Sci. USA* **117**, 20438–20446 (2020).
7. Lasslop, G. et al. Global ecosystems and fire: multi-model assessment of fire-induced tree-cover and carbon storage reduction. *Glob. Change Biol.* **26**, 5027–5041 (2020).
8. Xu, C. et al. Increasing impacts of extreme droughts on vegetation productivity under climate change. *Nat. Clim. Chang.* **9**, 948–953 (2019).
9. Booth, B. B. B. et al. High sensitivity of future global warming to land carbon cycle processes. *Environ. Res. Lett.* **7**, 024002 (2012).
10. Huntingford, C. et al. Implications of improved representations of plant respiration in a changing climate. *Nat. Commun.* **8**, 1602 (2017).
11. Farquhar, G. D., Caemmerer, S. & Berry, J. A biochemical model of photosynthetic CO₂ assimilation in leaves of C3 species. *Planta* **149**, 78–90 (1980).
12. Atkin, O. K. et al. Leaf respiration in terrestrial biosphere models. in *Plant Respiration: Metabolic Fluxes and Carbon Balance, Advances in Photosynthesis and Respiration* Ch. 6, 107–142 (Springer, 2017).
13. Arcus, V. L. et al. On the temperature dependence of enzyme-catalyzed rates. *Biochemistry* **55**, 1681–1688 (2016).
14. Hobbs, J. K. et al. Change in heat capacity for enzyme catalysis determines temperature dependence of enzyme catalyzed rates. *ACS Chem. Biol.* **8**, 2388–2393 (2013).

15. Prentice, E. et al. The inflection point hypothesis: the relationship between the temperature dependence of enzyme catalyzed reaction rates and microbial growth rates. *Biochemistry* **59**, 3562–3569 (2020).
16. Ratkowsky, D. A., Olley, J. & Ross, T. Unifying temperature effects on the growth rate of bacteria and the stability of globular proteins. *J. Theor. Biol.* **233**, 351–362 (2005).
17. Corkrey, R. et al. Universality of thermodynamic constants governing biological growth rates. *PLoS ONE* **7**, e32003 (2012).
18. García, F. C. et al. The temperature dependence of microbial community respiration is amplified by changes in species interactions. *Nat. Microbiol.* **8**, 272–283 (2023).
19. Alster, C. J. et al. Quantifying thermal adaptation of soil microbial respiration. *Nat. Commun.* **14**, 5459 (2023).
20. Kruse, J., Rennenberg, H. & Adams, M. A. Three physiological parameters capture variation in leaf respiration of *Eucalyptus grandis*, as elicited by short-term changes in ambient temperature, and differing nitrogen supply. *Plant Cell Environ.* <https://doi.org/10.1111/pce.13162> (2018).
21. Liang, L. L. et al. Macromolecular rate theory (MMRT) provides a thermodynamics rationale to underpin the convergent temperature response in plant leaf respiration. *Glob. Change Biol.* **24**, 1538–1547 (2018).
22. O'Sullivan, O. S. et al. High-resolution temperature responses of leaf respiration in snow gum (*Eucalyptus pauciflora*) reveal high-temperature limits to respiratory function. *Plant Cell Environ.* **36**, 1268–1284 (2013).
23. O'Sullivan, O. S. et al. Thermal limits of leaf metabolism across biomes. *Glob. Change Biol.* **23**, 209–223 (2017).
24. Carey, J. C. et al. Temperature response of soil respiration largely unaltered with experimental warming. *Proc. Natl Acad. Sci. USA* **113**, 13797–13802 (2016).
25. Numa, K. B., Robinson, J. M., Arcus, V. L. & Schipper, L. A. Separating the temperature response of soil respiration derived from soil organic matter and added labile carbon compounds. *Geoderma* **400**, 115128 (2021).
26. Schipper, L. A., Hobbs, J. K., Rutledge, S. & Arcus, V. L. Thermodynamic theory explains the temperature optima of soil microbial processes and high Q_{10} values at low temperatures. *Glob. Change Biol.* **20**, 3578–3586 (2014).
27. Chen, W. et al. Evidence for widespread thermal optimality of ecosystem respiration. *Nat. Ecol. Evol.* **7**, 1379–1387 (2023).
28. Varney, R. M., Chadburn, S. E., Burke, E. J. & Cox, P. M. Evaluation of soil carbon simulation in CMIP6 Earth system models. *Biogeosciences* **19**, 4671–4704 (2022).
29. Todd-Brown, K. E. O. et al. Causes of variation in soil carbon simulations from CMIP5 Earth system models and comparison with observations. *Biogeosciences* **10**, 1717–1736 (2013).
30. Hou, E. et al. Across-model spread and shrinking in predicting peatland carbon dynamics under global change. *Glob. Change Biol.* **29**, 2759–2775 (2023).
31. Arrhenius, S. Über die Dissociationswärme und den Einfluss der Temperatur auf den Dissociationsgrad der Elektrolyte. *Z. für Physikalische Chem.* **4U**, 96–116 (1889).
32. Lloyd, J. & Taylor, J. A. On the temperature dependence of soil respiration. *Funct. Ecol.* **8**, 315–323 (1994).
33. Davidson, E. A., Savage, K. E. & Finzi, A. C. A big-microsite framework for soil carbon modeling. *Glob. Change Biol.* **20**, 3610–3620 (2014).
34. Del Grosso, S. J. et al. Modeling soil CO₂ emissions from ecosystems. *Biogeochemistry* **73**, 71–91 (2005).
35. Arroyo, J. I., Diez, B., Kempes, C. P., West, G. B. & Marquet, P. A. A general theory for temperature dependence in biology. *Proc. Natl Acad. Sci. USA* **119**, e2119872119 (2022).
36. Tang, J. & Riley, W. J. A reanalysis of the foundations of the macromolecular rate theory. *Biogeosci. Discuss.* <https://doi.org/10.5194/bg-2023-77> (2023).
37. Zhang, W. et al. Soil moisture and atmospheric aridity impact spatio-temporal changes in evapotranspiration at a global scale. *J. Geophys. Res. Atmos.* **128**, e2022JD038046 (2023).
38. Davidson, E. A., Samanta, S., Caramori, S. S. & Savage, K. The Dual Arrhenius and Michaelis–Menten kinetics model for decomposition of soil organic matter at hourly to seasonal time scales. *Glob. Change Biol.* **18**, 371–384 (2012).
39. Bunnell, F. L., Tait, D. E. N., Flanagan, P. W. & Van Clever, K. Microbial respiration and substrate weight loss — I: a general model of the influences of abiotic variables. *Soil. Biol. Biochem.* **9**, 33–40 (1977).
40. Davidson, E. A. & Janssens, I. A. Temperature sensitivity of soil carbon decomposition and feedbacks to climate change. *Nature* **440**, 165–173 (2006).
41. Mahecha, M. D. et al. Global convergence in the temperature sensitivity of respiration at ecosystem level. *Science* **329**, 838–840 (2010).
42. Michaletz, S. T. & Garen, J. C. Hotter is not (always) better: embracing unimodal scaling of biological rates with temperature. *Ecol. Lett.* **27**, e14381 (2024).
43. Smith, J. M. Group selection and kin selection. *Nature* **201**, 1145–1147 (1964).
44. Atkin, O. K., Scheurwater, I. & Pons, T. L. Respiration as a percentage of daily photosynthesis in whole plants is homeostatic at moderate, but not high, growth temperatures. *N. Phytol.* **174**, 367–380 (2007).
45. Ryan, M. G., Linder, S., Vose, J. M. & Hubbard, R. M. Dark respiration of pines. *Ecol. Bull.* **43**, 50–63 (1994).
46. Bruhn, D. et al. Nocturnal plant respiration is under strong non-temperature control. *Nat. Commun.* **13**, 5650 (2022).
47. Heskell, M. A. et al. Convergence in the temperature response of leaf respiration across biomes and plant functional types. *Proc. Natl Acad. Sci. USA* **113**, 3832–3837 (2016).
48. Zhu, L. et al. Acclimation of leaf respiration temperature responses across thermally contrasting biomes. *N. Phytol.* **229**, 1312–1325 (2021).
49. Tjoelker, M. G., Oleksyn, J. & Reich, P. B. Modelling respiration of vegetation: evidence for a general temperature-dependent Q_{10} . *Glob. Change Biol.* **7**, 223–230 (2001).
50. Kurepin, L. V. et al. Contrasting acclimation abilities of two dominant boreal conifers to elevated CO₂ and temperature. *Plant. Cell Environ.* **41**, 1331–1345 (2018).
51. Atkin, O. K. & Tjoelker, M. G. Thermal acclimation and the dynamic response of plant respiration to temperature. *Trends Plant Sci.* **8**, 343–351 (2003).
52. Smith, N. G. & Dukes, J. S. Plant respiration and photosynthesis in global-scale models: incorporating acclimation to temperature and CO₂. *Glob. Change Biol.* **19**, 45–63 (2013).
53. Amthor, J. S. The role of maintenance respiration in plant growth. *Plant Cell Environ.* **7**, 561–569 (1984).
54. Dusenke, M. E., Duarte, A. G. & Way, D. A. Plant carbon metabolism and climate change: elevated CO₂ and temperature impacts on photosynthesis, photorespiration and respiration. *N. Phytol.* **221**, 32–49 (2019).
55. Scafaro, A. P. et al. Responses of leaf respiration to heatwaves. *Plant Cell Environ.* **44**, 2090–2101 (2021).
56. Hüve, K., Bichele, I., Rasulov, B. & Niinemets, U. When it is too hot for photosynthesis: heat-induced instability of photosynthesis in relation to respiratory burst, cell permeability changes and H₂O₂ formation. *Plant Cell Environ.* **34**, 113–126 (2011).
57. Hüve, K. et al. Temperature responses of dark respiration in relation to leaf sugar concentration. *Physiol. Plant* **144**, 320–334 (2012).
58. Schmiege, S. C., Heskell, M., Fan, Y. & Way, D. A. It's only natural: plant respiration in unmanaged systems. *Plant Physiol.* **192**, 710–727 (2023).
59. Zhu, J., Wu, Q., Wu, F. & Ni, X. Partitioning of root, litter and microbial respiration by plant input manipulation in forests. *Environ. Res. Lett.* **18**, 024043 (2023).
60. Bond-Lamberty, B. et al. Twenty years of progress, challenges, and opportunities in measuring and understanding soil respiration. *J. Geophys. Res. Biogeosci.* **129**, e2023JG007637 (2024).
61. Wang, X. et al. Soil respiration under climate warming: differential response of heterotrophic and autotrophic respiration. *Glob. Change Biol.* **20**, 3229–3237 (2014).
62. Patel, K. F. et al. Carbon flux estimates are sensitive to data source: a comparison of field and lab temperature sensitivity data. *Environ. Res. Lett.* **17**, 113003 (2022).
63. Li, D., Zhou, X., Wu, L., Zhou, J. & Luo, Y. Contrasting responses of heterotrophic and autotrophic respiration to experimental warming in a winter annual-dominated prairie. *Glob. Change Biol.* **19**, 3553–3564 (2013).
64. Bradford, M. A. et al. Thermal adaptation of soil microbial respiration to elevated temperature. *Ecol. Lett.* **11**, 1316–1327 (2008).
65. Yergeau, E. et al. Shifts in soil microorganisms in response to warming are consistent across a range of Antarctic environments. *ISME J.* **6**, 692–702 (2012).
66. Luo, C. et al. Soil microbial community responses to a decade of warming as revealed by comparative metagenomics. *Appl. Environ. Microbiol.* **80**, 1777–1786 (2014).
67. Allison, S. D., Wallenstein, M. D. & Bradford, M. A. Soil-carbon response to warming dependent on microbial physiology. *Nat. Geosci.* **3**, 336–340 (2010).
68. Kirschbaum, M. U. F. Soil respiration under prolonged soil warming: are rate reductions caused by acclimation or substrate loss? *Glob. Change Biol.* **10**, 1870–1877 (2004).
69. Knorr, W., Prentice, I. C., House, J. I. & Holland, E. A. Long-term sensitivity of soil carbon turnover to warming. *Nature* **433**, 298–301 (2005).
70. Conant, R. T. et al. Sensitivity of organic matter decomposition to warming varies with its quality. *Glob. Change Biol.* **14**, 868–877 (2008).
71. Li, Y. et al. Microbial community responses reduce soil carbon loss in Tibetan alpine grasslands under short-term warming. *Glob. Change Biol.* **25**, 3438–3449 (2019).
72. Parton, W. J., Schimel, D. S., Cole, C. V. & Ojima, D. S. Analysis of factors controlling soil organic matter levels in Great Plains grasslands. *Soil. Sci. Soc. Am. J.* **51**, 1173–1179 (1987).
73. Liu, Y. et al. The optimum temperature of soil microbial respiration: patterns and controls. *Soil Biol. Biochem.* **121**, 35–42 (2018).
74. Parker, L. W., Miller, J., Steinberger, Y. & Whitford, W. G. Soil respiration in a chihuahuan desert rangeland. *Soil Biol. Biochem.* **15**, 303–309 (1983).
75. Richardson, J., Chatterjee, A. & Darrel Jenerette, G. Optimum temperatures for soil respiration along a semi-arid elevation gradient in southern California. *Soil Biol. Biochem.* **46**, 89–95 (2012).
76. Pietikäinen, J., Pettersson, M. & Bååth, E. Comparison of temperature effects on soil respiration and bacterial and fungal growth rates. *FEMS Microbiol. Ecol.* **52**, 49–58 (2005).
77. Balsler, T. C. & Wixon, D. L. Investigating biological control over soil carbon temperature sensitivity. *Glob. Change Biol.* **15**, 2935–2949 (2009).
78. Makita, N., Fujimoto, R. & Tamura, A. The contribution of roots, mycorrhizal hyphae, and soil free-living microbes to soil respiration and its temperature sensitivity in a larch forest. *Forests* **12**, 1410 (2021).
79. Lelley-Kovács, E. et al. Thresholds and interactive effects of soil moisture on the temperature response of soil respiration. *Eur. J. Soil Biol.* **47**, 247–255 (2011).
80. Alster, C. J., Koyama, A., Johnson, N. G., Wallenstein, M. D. & von Fischer, J. C. Temperature sensitivity of soil microbial communities: an application of macromolecular rate theory to microbial respiration. *J. Geophys. Res. Biogeosci.* **121**, 1420–1433 (2016).
81. Alster, C. J., von Fischer, J. C., Allison, J. C. & Treseder, K. K. Embracing a new paradigm for temperature sensitivity of soil microbes. *Glob. Change Biol.* **26**, 3221–3229 (2020).
82. Trumbore, S. Carbon respired by terrestrial ecosystems — recent progress and challenges. *Glob. Change Biol.* **12**, 141–153 (2006).
83. Reichstein, M. et al. On the separation of net ecosystem exchange into assimilation and ecosystem respiration: review and improved algorithm. *Glob. Change Biol.* **11**, 1424–1439 (2005).

84. Lasslop, G. et al. Separation of net ecosystem exchange into assimilation and respiration using a light response curve approach: critical issues and global evaluation. *Glob. Change Biol.* **16**, 187–208 (2010).
85. Davidson, E. A., Richardson, A. D., Savage, K. E. & Hollinger, D. Y. A distinct seasonal pattern of the ratio of soil respiration to total ecosystem respiration in a spruce-dominated forest. *Glob. Change Biol.* **12**, 230–239 (2006).
86. Barba, J. et al. Comparing ecosystem and soil respiration: review and key challenges of tower-based and soil measurements. *Agric. For. Meteorol.* **249**, 434–443 (2018).
87. Yvon-Durocher, G. et al. Reconciling the temperature dependence of respiration across timescales and ecosystem types. *Nature* **487**, 472–476 (2012).
88. Drewitt, G. et al. Measuring forest floor CO₂ fluxes in a Douglas-fir forest. *Agric. For. Meteorol.* **110**, 299–317 (2002).
89. Lafleur, P. M., Moore, T., Roulet, N. & Frokling, S. Ecosystem respiration in a cool temperate bog depends on peat temperature but not water table. *Ecosystems* **8**, 619–629 (2005).
90. Ma, W. et al. Carbon budgets and environmental controls in alpine ecosystems on the Qinghai-Tibet Plateau. *Catena* **229**, 107224 (2023).
91. Lin, X. et al. Response of ecosystem respiration to warming and grazing during the growing seasons in the alpine meadow on the Tibetan plateau. *Agric. For. Meteorol.* **151**, 792–802 (2011).
92. Wen, X. et al. Soil moisture effect on the temperature dependence of ecosystem respiration in a subtropical *Pinus* plantation of southeastern China. *Agric. For. Meteorol.* **137**, 166–175 (2006).
93. Wagle, P. Confounding effects of soil moisture on the relationship between ecosystem respiration and soil temperature in switchgrass. *BioEnergy Res.* **7**, 789–798 (2014).
94. Jia, X. et al. Seasonal and interannual variations in ecosystem respiration in relation to temperature, moisture, and productivity in a temperate semi-arid shrubland. *Sci. Total Environ.* **709**, 136210 (2020).
95. Gu, L., Hanson, P. J., Mac Post, W. & Liu, Q. A novel approach for identifying the true temperature sensitivity from soil respiration measurements. *Glob. Biogeochem. Cycles* **22**, GB4009 (2008).
96. Xu, X. et al. Plant community structure regulates responses of prairie soil respiration to decadal experimental warming. *Glob. Change Biol.* **21**, 3846–3853 (2015).
97. Wu, D. et al. Evaluation of the intrinsic temperature sensitivity of ecosystem respiration in typical ecosystems of an endorheic river basin. *Agric. For. Meteorol.* **333**, 109393 (2023).
98. Kirschbaum, M. U. F. Seasonal variations in the availability of labile substrate confound the temperature dependence of organic matter decomposition. *Soil Biol. Biochem.* **57**, 568–576 (2013).
99. Smith, N. G. & Dukes, J. S. Short-term acclimation to warmer temperatures accelerates leaf carbon exchange processes across plant types. *Glob. Change Biol.* **23**, 4840–4853 (2017).
100. Atkin, O. K., Scheurwater, I. & Pons, T. L. High thermal acclimation potential of both photosynthesis and respiration in two lowland *Plantago* species in contrast to an alpine congener. *Glob. Change Biol.* **12**, 500–515 (2006).
101. Cable, J. M. et al. The temperature responses of soil respiration in deserts: a seven desert synthesis. *Biogeochemistry* **103**, 71–90 (2011).
102. Vanderwel, M. C. et al. Global convergence in leaf respiration from estimates of thermal acclimation across time and space. *N. Phytol.* **207**, 1026–1037 (2015).
103. Wen, X.-F., Wang, H.-M., Wang, J.-L., Yu, G.-R. & Sun, X.-M. Ecosystem carbon exchanges of a subtropical evergreen coniferous forest subjected to seasonal drought, 2003–2007. *Biogeosciences* **7**, 357–369 (2010).
104. Fanin, N. et al. Soil enzymes in response to climate warming: mechanisms and feedbacks. *Funct. Ecol.* **36**, 1378–1395 (2022).
105. Niu, B. et al. Warming homogenizes apparent temperature sensitivity of ecosystem respiration. *Sci. Adv.* **7**, eabc7358 (2021).
106. Liu, T., Xu, Z.-Z., Hou, Y.-H. & Zhou, G.-S. Effects of warming and changing precipitation rates on soil respiration over two years in a desert steppe of northern China. *Plant Soil* **400**, 15–27 (2016).
107. Tucker, C. L. & Reed, S. C. Low soil moisture during hot periods drives apparent negative temperature sensitivity of soil respiration in a dryland ecosystem: a multi-model comparison. *Biogeochemistry* **128**, 155–169 (2016).
108. Crous, K. Y., Uddling, J. & De Kauwe, M. G. Temperature responses of photosynthesis and respiration in evergreen trees from boreal to tropical latitudes. *N. Phytol.* **234**, 353–374 (2022).
109. Yang, Z. et al. Recent photosynthates are the primary carbon source for soil microbial respiration in subtropical forests. *Geophys. Res. Lett.* **49**, e2022GL101147 (2022).
110. Wang, B. et al. Dryness limits vegetation pace to cope with temperature change in warm regions. *Glob. Change Biol.* **29**, 4750–4757 (2023).
111. Baldocchi, D. D. How eddy covariance flux measurements have contributed to our understanding of global change biology. *Glob. Change Biol.* **26**, 242–260 (2020).
112. Pastorello, G. et al. The FLUXNET2015 dataset and the ONEflux processing pipeline for eddy covariance data. *Sci. Data* **7**, 225 (2020).
113. Luo, Y., Wan, S., Hui, D. & Wallace, L. L. Acclimatization of soil respiration to warming in a tall grass prairie. *Nature* **413**, 622–625 (2001).
114. Loveys, B. R. et al. Thermal acclimation of leaf and root respiration: an investigation comparing inherently fast- and slow-growing plant species. *Glob. Change Biol.* **9**, 895–910 (2003).
115. Wright, I. J. et al. Irradiance, temperature and rainfall influence leaf dark respiration in woody plants: evidence from comparisons across 20 sites. *N. Phytol.* **169**, 309–319 (2006).
116. Tjoelker, M. G., Oleksyn, J., Lorenc-Plucinska, G. & Reich, P. B. Acclimation of respiratory temperature responses in northern and southern populations of *Pinus banksiana*. *N. Phytol.* **181**, 218–229 (2009).
117. Mujawariya, M. et al. Complete or overcompensatory thermal acclimation of leaf dark respiration in African tropical trees. *N. Phytol.* **229**, 2548–2561 (2021).
118. Luo, Y. et al. Matrix approach to land carbon cycle modeling. *J. Adv. Model. Earth Syst.* **14**, e2022MS003008 (2022).
119. Wei, N. et al. Evolution of uncertainty in terrestrial carbon storage in Earth System Models from CMIP5 to CMIP6. *J. Clim.* **35**, 5483–5499 (2022).
120. Guenet, B. et al. Spatial biases reduce the ability of Earth System Models to simulate soil heterotrophic respiration fluxes. *EGU Sphere* <https://doi.org/10.5194/egusphere-2023-922> (2023).
121. Xia, J. et al. Terrestrial ecosystem model performance in simulating productivity and its vulnerability to climate change in the northern permafrost region. *J. Geophys. Res. Biogeosci.* **122**, 430–446 (2017).
122. Krinner, G. et al. A dynamic global vegetation model for studies of the coupled atmosphere–biosphere system. *Glob. Biogeochem. Cycles* **19**, GB1015 (2005).
123. Cox, P. Description of the TRIFFID dynamic global vegetation model. *Hadley Centre Technical Note 24* (2001).
124. Lawrence, D. M. et al. The Community Land Model Version 5: description of new features, benchmarking, and impact of forcing uncertainty. *J. Adv. Model. Earth Syst.* **11**, 4245–4287 (2019).
125. Xia, J., Wang, J. & Niu, S. Research challenges and opportunities for using big data in global change biology. *Glob. Change Biol.* **26**, 6040–6061 (2020).
126. Ping, J. et al. Enhanced causal effect of ecosystem photosynthesis on respiration during heatwaves. *Sci. Adv.* **9**, eadi6395 (2023).
127. Xia, J., Luo, Y., Wang, Y.-P. & Hararuk, O. Traceable components of terrestrial carbon storage capacity in biogeochemical models. *Glob. Change Biol.* **19**, 2104–2116 (2013).
128. Wei, N. et al. Nutrient limitations lead to a reduced magnitude of disequilibrium in the global terrestrial carbon cycle. *J. Geophys. Res. Biogeosci.* **127**, e2021JG006764 (2022).
129. Luo, Y. & Schuur, E. A. G. Model parameterization to represent processes at unresolved scales and changing properties of evolving systems. *Glob. Change Biol.* **26**, 1109–1117 (2020).
130. Li, Q. et al. Variation of parameters in a flux-based ecosystem model across 12 sites of terrestrial ecosystems in the conterminous USA. *Ecol. Model.* **336**, 57–69 (2016).
131. Tao, F. et al. Deep learning optimizes data-driven representation of soil organic carbon in Earth System Model over the conterminous United States. *Front. Big Data* **3**, 17 (2020).
132. Liang, J. et al. More replenishment than priming loss of soil organic carbon with additional carbon input. *Nat. Commun.* **9**, 3175 (2018).
133. Liao, C. et al. Microbe–iron interactions control lignin decomposition in soil. *Soil Biol. Biochem.* **173**, 108803 (2022).
134. Luo, Y. et al. Elevated CO₂ differentiates ecosystem carbon processes: deconvolution analysis of Duke Forest Face Data. *Ecol. Monogr.* **71**, 357–376 (2001).
135. Luo, Y. Terrestrial carbon–cycle feedback to climate warming. *Annu. Rev. Ecol. Evol. Syst.* **38**, 683–712 (2007).
136. Miner, K. R. et al. Permafrost carbon emissions in a changing Arctic. *Nat. Rev. Earth Environ.* **3**, 55–67 (2022).
137. Schuur, E. A. G. et al. Climate change and the permafrost carbon feedback. *Nature* **520**, 171–179 (2015).
138. Nottingham, A. T., Gloor, E., Bååth, E. & Meir, P. Soil carbon and microbes in the warming tropics. *Funct. Ecol.* **36**, 1338–1354 (2022).
139. Nottingham, A. et al. Microbial diversity declines in warmed tropical soil and respiration rise exceed predictions as communities adapt. *Nat. Microbiol.* **7**, 1–11 (2022).
140. Atkin, O. K. et al. Global variability in leaf respiration in relation to climate, plant functional types and leaf traits. *N. Phytol.* **206**, 614–636 (2015).
141. Jagadish, S. V. K., Way, D. A. & Sharkey, T. D. Scaling plant responses to high temperature from cell to ecosystem. *Plant Cell Environ.* **44**, 1987–1991 (2021).
142. Luo, Y. et al. Sustainability of terrestrial carbon sequestration: a case study in Duke Forest with inversion approach. *Glob. Biogeochem. Cycles* **17**, 1021 (2003).
143. Moyano, F. E., Manzoni, S. & Chenu, C. Responses of soil heterotrophic respiration to moisture availability: an exploration of processes and models. *Soil Biol. Biochem.* **59**, 72–85 (2013).
144. Linn, D. M. & Doran, J. W. Effect of water-filled pore space on carbon dioxide and nitrous oxide production in tilled and nontilled soils. *Soil Sci. Soc. Am. J.* **48**, 1267–1272 (1984).

Acknowledgements

This work was supported by the National Natural Science Foundation of China (31988102), the National Key Technology R & D Program of China (2022YFF0802102) and the International Partnership Program of the Chinese Academy of Science (177GJHZ2022020BS).

Author contributions

S.N. conceived the ideas and designed the study framework. S.N., W.C., L.L.L., C.A.S., J.X., M.H., K.F.P. and B.B.-L. led the writing of the manuscript. S.W. and J.W. assisted with data collation and figures. M.U.F.K., O.K.A., G.Y.-D., Y.H. and Y.L. helped to improve the writing of the paper and contributed to the revisions. All authors contributed to the drafts and revision.

Competing interests

The authors declare no competing interests.

Additional information

Supplementary information The online version contains supplementary material available at <https://doi.org/10.1038/s43017-024-00569-3>.

Peer review information *Nature Reviews Earth & Environment* thanks Mark Tjoelker, Holger Lange and the other, anonymous, reviewer(s) for their contribution to the peer review of this work.

Publisher's note Springer Nature remains neutral with regard to jurisdictional claims in published maps and institutional affiliations.

Springer Nature or its licensor (e.g. a society or other partner) holds exclusive rights to this article under a publishing agreement with the author(s) or other rightsholder(s); author self-archiving of the accepted manuscript version of this article is solely governed by the terms of such publishing agreement and applicable law.

© Springer Nature Limited 2024

¹Key Laboratory of Ecosystem Network Observation and Modeling, Institute of Geographic Sciences and Natural Resources Research, Chinese Academy of Sciences, Beijing, China. ²College of Resources and Environment, University of Chinese Academy of Sciences, Beijing, China. ³Manaaki Whenua — Landcare Research, Palmerston North, New Zealand. ⁴Max Planck Institute for Biogeochemistry, Jena, Germany. ⁵Research Center for Global Change and Complex Ecosystems, School of Ecological and Environmental Sciences, East China Normal University, Shanghai, China. ⁶Department of Biology, Macalester College, Saint Paul, MN, USA. ⁷Pacific Northwest National Laboratory, Richland, WA, USA. ⁸Joint Global Change Research Institute, Pacific Northwest National Laboratory, College Park, MD, USA. ⁹Environment and Sustainability Institute, University of Exeter, Penryn, UK. ¹⁰Division of Plant Sciences, Research School of Biology, Australian National University, Canberra, Australian Capital Territory, Australia. ¹¹Soil and Crop Sciences Section, School of Integrative Plant Science, Cornell University, Ithaca, NY, USA.